

Pulsed airborne lidar measurements of CO₂ column absorption

James B. Abshire¹, Haris Riris¹, Graham R. Allan², Clark J. Weaver³, Jianping Mao³, Xiaoli Sun¹, William E. Hasselbrack², Michael Rodriguez², Edward V. Browell⁴

¹*NASA Goddard Space Flight Center, Greenbelt, MD 20771, USA*

²*Sigma Space Inc., Lanham, MD 20706 USA*

³*Goddard Earth Sciences and Technology Center, UMBC, Baltimore, MD 21228, USA*

⁴*NASA Langley Research Center, Hampton VA 23681, USA*

Keywords: Space lidar, CO₂, Airborne lidar, Differential Absorption Lidar

ABSTRACT

We report on airborne lidar measurements of atmospheric CO₂ column density for an approach being developed as a candidate for NASA's ASCENDS mission. It uses a pulsed dual-wavelength lidar measurement based on the integrated path differential absorption (IPDA) technique. We demonstrated the approach using the CO₂ measurement from aircraft in July and August 2009 over four locations. The results show clear CO₂ line shape and absorption signals, which follow the expected changes with aircraft altitude from 3 to 13 km. The 2009 measurements have been analyzed in detail and the results show ~1 ppm random errors for 8-10 km altitudes and ~30 sec averaging times. Airborne measurements were also made in 2010 with stronger signals and initial analysis shows ~0.3 ppm random errors for 80 sec averaging times for altitudes >6 km.

1. INTRODUCTION

The US National Research Council's 2007 Decadal Survey for Earth Science recommended a space-based CO₂ measuring mission called ASCENDS [1]. Its goals are to produce global atmospheric CO₂ measurements using the laser absorption spectroscopy approach. ASCENDS will allow continuous measurements over the cloud-free oceans, at low sun angles and in darkness, which are major advantages over passive sensors [2].

2. LIDAR APPROACH

Our group has developed a pulsed lidar approach, shown in Figure 1, as a candidate for the ASCENDS mission [3-5]. It uses a dual band pulsed laser absorption spectrometer and the integrated path differential absorption (IPDA) lidar technique. The approach uses two tunable pulsed laser transmitters allowing simultaneous measurement of the absorption from a CO₂ absorption line in the 1570 nm band, O₂ extinction in the oxygen A-band, and surface height and atmospheric backscatter in the same path. A tunable laser is stepped in wavelength across a single CO₂ line for the CO₂ column measurement, while simultaneously a laser is stepped across a line doublet near 765 nm in the Oxygen A-band for an atmospheric pressure measurement [6]. Both lasers are pulsed at a ~8kHz rate, and the two absorption line regions are sampled in wavelength

steps at typically ~1 KHz. The direct detection receiver measures the time resolved laser backscatter from the atmosphere along with the energies of the laser echoes from the surface. After suitable averaging the gas extinction and column densities for the CO₂ and O₂ gases are estimated from the sampled wavelengths of the surface reflected line shapes via the Integrated Path Differential Absorption (IPDA) Lidar technique [7].

Our approach measures a single CO₂ line in the 1570 nm band [8]. The centermost line of R-branch at 1572.335 nm, shown in Figure 1, has been analyzed and is an attractive line for CO₂ measurements [23]. Our concept for space measures the CO₂ lineshape at 8 wavelengths. This allows for solving for wavelength offsets via a line fitting process. The distributed wavelength sampling across the line region also allows the instrument's response to be characterized as a function of wavelength, which allows modeling to reduce the impact of wavelength dependent responses. Using pulsed lasers and receiver processing to range resolve the laser backscatter profiles also allows post detection signal processing to isolate the laser echo signals from the surface, and to reject laser photons scattered from the atmosphere. This also substantially improves the receiver's SNR by reducing the amount of noise admitted from the detector and the solar background.

3. 2009 AIRBORNE LIDAR

In 2008 we first demonstrated airborne lidar measurements on the NASA Glenn Lear-25 aircraft [3] shown in Figure 2. A laser signal drawing and lidar block diagram are shown in Figure 3. The lidar signal source is a DFB laser diode, which is operated near 1572.33 nm by controlling its temperature and current. A ramp from a signal generator was used to sweep the current to the diode laser, and hence its output wavelength. The diode's CW output is then gated into pulses using an acousto-optic modulator (AOM) to an Erbium Doped Fiber Amplifier

(EDFA). A small percentage of the CW seed laser output is split off and directed through a fiber-coupled CO₂ absorption cell and to a PIN detector. The CO₂ cell serves as a monitor for center wavelength of the sweep. The nominal static transmitted laser pulse wavelengths are measured in a calibration procedure using a commercial wavemeter. Subsequent testing showed some curvature in the scanning dynamic ramp signal, so we used a more accurate quadratic functional model for the laser wavelength vs pulse position in the data analysis.



Figure 1- *Left* - NASA Glenn Lear-25 aircraft. The nadir window assembly is just below the NASA logo. Photographs of the lidar installed on the aircraft showing the sensor head assembly (*Middle*) and the dual aircraft racks (*Right*).

Table 1 – 2009 Pulsed Airborne CO₂ Lidar Parameters

| | | | |
|--|-----------------------------------|------------------------------|-------------------------------|
| CO ₂ line center wavelength | 1572.33 nm (typically) | Telescope diameter | 20 cm |
| Laser min & max wavelengths | 1572.29 nm, 1572.39 nm | Receiver FOV diameter | 200 μ rad |
| Laser wavelength steps across line | 20 (these flights) | Receiver optical bandwidth | 800 pm FWHM |
| Laser wavelength change/step | ~ 5 pm | Receiver Optics Transmission | 64% |
| Laser peak power, pulse width, energy | 25 watts, 1 μ sec, 25 μ J | Detector PMT type | Hamamatsu H10330A-75 |
| Laser divergence angle | 100 μ rad (these flights) | Detector quantum efficiency | 2% (this device) |
| Seed laser diode type | DFB: Fitel FOL15DCWD | Detector dark count rate | ~ 500 kHz |
| Laser Pulse Modulator (AOM) | NEOS Model: 26035-2-155 | Receiver signal processing | Photon counting/histogramming |
| Fiber coupled CO ₂ cell | 80 cm path, ~200 Torr pressure | Histogram time bin width | 8 nsec |
| Fiber Laser Amplifier (EDFA) | IPG EAR-10K-1571-LP-SF | Receiver integration time | 1 second per readout |
| Laser line scan rate | 450 Hz | Recording duty cycle | 50% (1 sec. every 2 sec.) |
| Laser linewidth per step | ~15 MHz | Instrument rack size & mass: | ~ 90 cm tall, total: 147 kg |
| Receiver Telescope type | Cassegrain, f/10 (Vixen) | Sensor head size and mass | ~ 25 x 60 x 60 cm, 41 kg |

The laser output is a sequence of 1usec-wide laser pulses which occur at a 10 KHz rate. The collimated transmitted laser signal exits through nadir aircraft window. The laser backscatter is collected by the receiver's 20 cm diameter Cassegrain telescope, which views nadir through the same window in a bistatic configuration. A multimode fiber is used to couple the optical signal from the telescope focal plane to the receiver optics. After passing through an optical bandpass filter, the signal is focused onto a PMT detector. The PMT used in the 2009 flights had a single photon counting efficiency of ~2%. The electrical pulse output from the PMT was amplified and passed through a threshold detector.

The pulses from the receiver's PMT detector and discriminator are binned and accumulated by the MCS. The start time of the MCS sweep is synchronized with the first laser pulse trigger and hence start of the pulsed wavelength sweep. Each MCS sweep contains a histogram of PMT pulse counts vs time for the wavelength sweeps (i.e. the laser backscatter profiles for all 20 pulses). At the end of 1 second, each bin contains the total receiver counts for the 450 laser sweeps. The receiver histogram record is then read and stored. The laser trigger and data acquisition is synchronized to timing markers from the GPS receiver and data is stored every other second. The computer also digitizes other signals, including those from, the inertial

guidance system output from the aircraft and GPS position and time. A nadir viewing video camera

4. 2009 AIRBORNE CAMPAIGNS

We used the NASA Glenn Lear-25 aircraft for the 2009 flights. The airborne lidar is configured into two half-racks and a “sensor head”, which contained the receiver telescope and the transmitter optics. A photograph of the sensor when integrated on the aircraft is shown in Figure 2. The sensor head was mounted above the lidar’s wedged and AR coated nadir viewing window assembly. During August 2009 we flew an airborne campaign with a series of 2.5 hour-long flights. We measured the shapes of the atmospheric CO₂ absorption line at stepped altitudes from 3-13 km over a variety of surfaces in the SGP ARM site, Illinois and near and over the Chesapeake Bay in North Carolina and eastern Virginia. Strong laser signals and clear CO₂ line shapes were observed at all altitudes on most flights, and some measurements were made through thin and broken clouds. These flights allowed testing and recording performance under different measurement conditions.

5. AIRBORNE CO₂ LIDAR MEASUREMENT PROCESSING

For the flights the lidar recorded the time- and wavelength-resolved laser backscatter with 1 second integration time. In subsequent analysis, the line shape measurements at each flight altitude step were averaged up to 10 sec. We used a CO₂ line retrieval approach based on the Gauss-Newton method to analyze each altitude averaged line shape. This approach has sufficient free parameters to model and correct for instrument effects, to fit the resulting CO₂ line shapes, and to estimate the corresponding CO₂ line optical depth at each altitude. The algorithm attempts to fit the sampled CO₂ line shape using a model with several sets of variables. The first is the reduction of the photon count ratio near the 1572.335 nm line due to CO₂ absorption. For these experiments the lidar’s wavelength (ie wavelength per laser pulse number) was modeled as a quadratic function, and the three wavelength coefficients were solved for, using the ground calibration as a prior constraint. The final set of variables modeled the changes in the lidar’s baseline response with wavelength. The CO₂ retrieval algorithm produces a set of parameters for each fit, including ones for signal strength, range to the surface and for differential optical depth (DOD) of the line peak.

also records the visible image through the window.

6. RESULTS

The CO₂ column absorption and range estimates [10] are analyzed for altitude step for each flight. We have conducted detailed analysis on the measurements of four flights in 2009, and the last flight in 2010. Some examples of the results are shown in Figures 3-7. More details and results from other flights, in 2009 and 2010, will be shown in the presentation.

7. SUMMARY

We have analyzed pulsed lidar measurements of CO₂ column density for four flights in August 2009. Three of the four flights were made in coordination with an ITT/LaRC lidar and a LaRC in-situ sensor [9], and were coordinated by Ed Browell of NASA LaRC. Some segments of these flights also demonstrated CO₂ line shapes measured through thin clouds. The lidar measurements were similar on all four flights. They showed the nearly the linear DOD vs altitude as calculated from atmospheric measurements and spectroscopy from HITRAN 2008. The scatter in the DOD was minimum in the 8-10 km altitude region, and had ~1 ppm random error there for 30 second averages.

The lidar’s configuration and settings were improved for the flights made in July 2010 from the NASA DC-8. For those flights the recorded lidar signals were almost 9 times stronger, and the CO₂ line sampling density was improved. The analysis for the last three 2010 flights to date shows improved measurement performance. The 2010 flight over the DOE ARM site showed 0.3 ppm random error over the 6-12 km altitude range using ~80 second averaging time. This corresponds to about 1.0 ppm errors for the 10 second averaging times targeted for a space mission. The analysis of these measurements will be completed in the summer 2011. In July 2010 we also demonstrated airborne O₂ column absorption measurements. Those measurements are being analyzed and will be reported in the future.

7. ACKNOWLEDGEMENTS

We are grateful for the support of the NASA Earth Science Technology Office’s Advanced Instrument Technology and Instrument Incubator Programs, the NASA ASCENDS Definition Program, and the Goddard IRAD program. We appreciate the excellent collaborations with NASA Glenn and Langley, and the in-situ atmospheric measurements from Ed Browell and Yonghoon Choi of NASA LaRC.

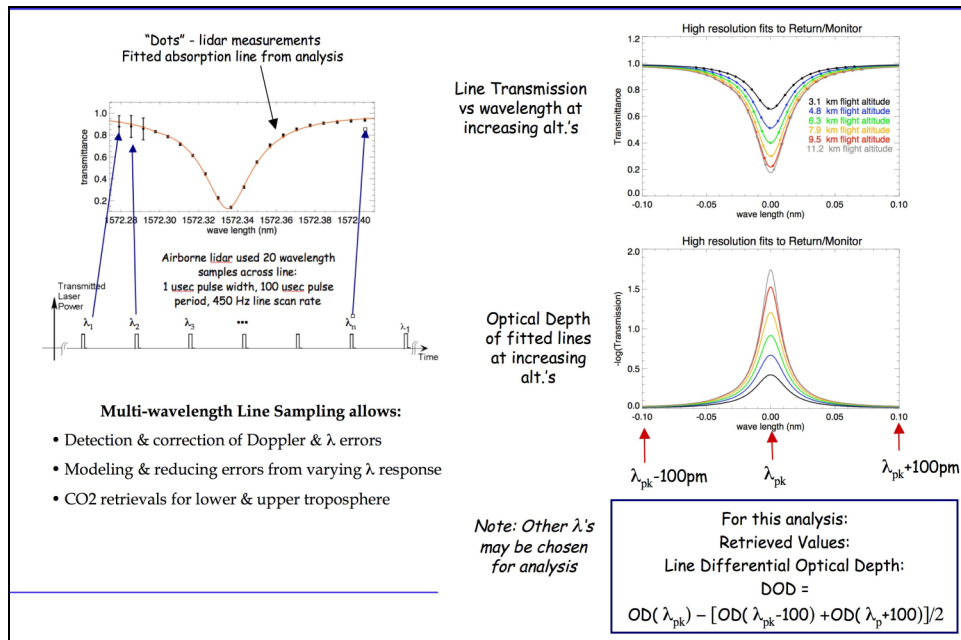


Figure 2- (left) The CO2 line sampling approach used in the 2009 flights. (Right top & middle) examples of fitted CO2 line shapes vs altitude. (Right bottom) Approach used to calculate the differential optical depth (DOD) of the fitted line.

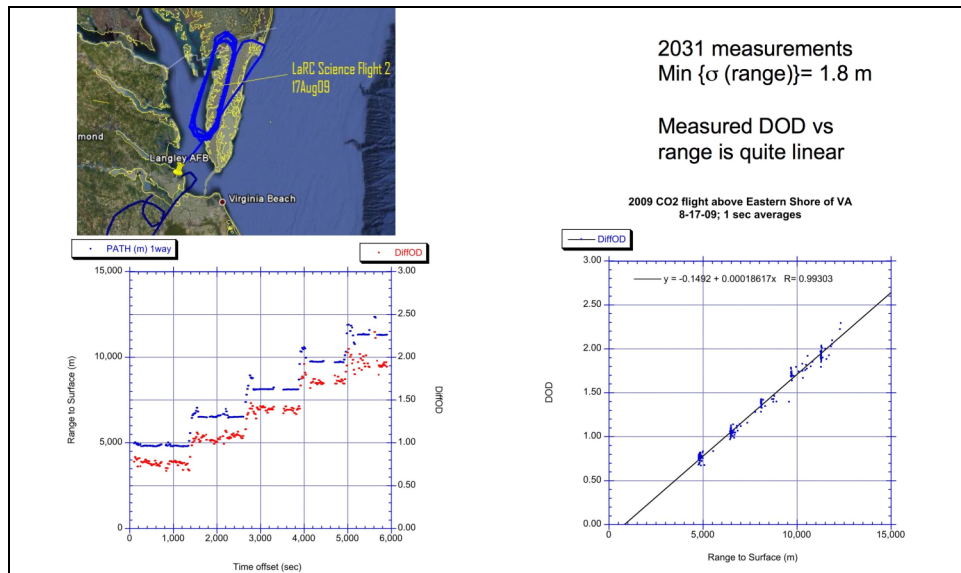


Figure 3 - Plots of the 1 second lidar measurements made above the Eastern Shore of VA the afternoon of August 17, 2009. (Left) plots of the measured range to the surface and DOD vs elapsed time. (Right) Scatter plot of the DOD vs range to the surface, and the best-fit line to the data. The distribution is quite linear, with more scatter above 10 km.

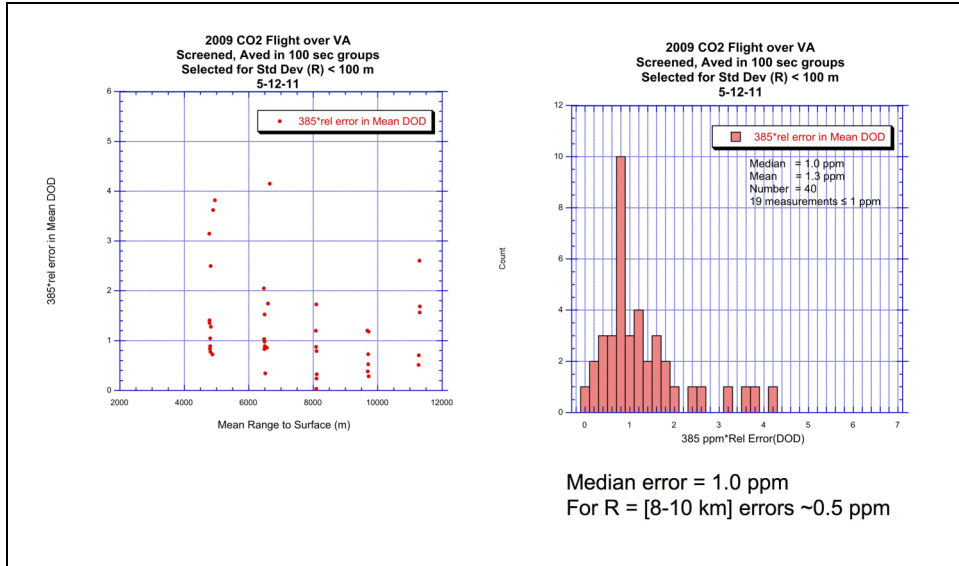


Figure 4- Summaries of scatter, or random error, in the groups of DOD values at constant ranges (those with rms altitude variability < 100 m) for the VA flight on August 17, 2009. The calculation approach is the same as the previous figure. (Left) Plots of the rms scatter in DOD values per group vs range to the surface. This curve is also U-shaped with minimum errors in the 8-9 km range. At smaller ranges, the relative error increases as the DOD decreases. At larger ranges, the relative error increases due to the smaller measured signals at the lidar due to $1/R^2$ losses and the increasing attenuation at line peak. (Right) Histogram of random errors at all altitudes. The median error for this flight was 1.0 ppm. The median error for this flight at all altitudes was 1.0 ppm. The minimum errors at the optimum 8-10 km range were ~0.5 ppm..

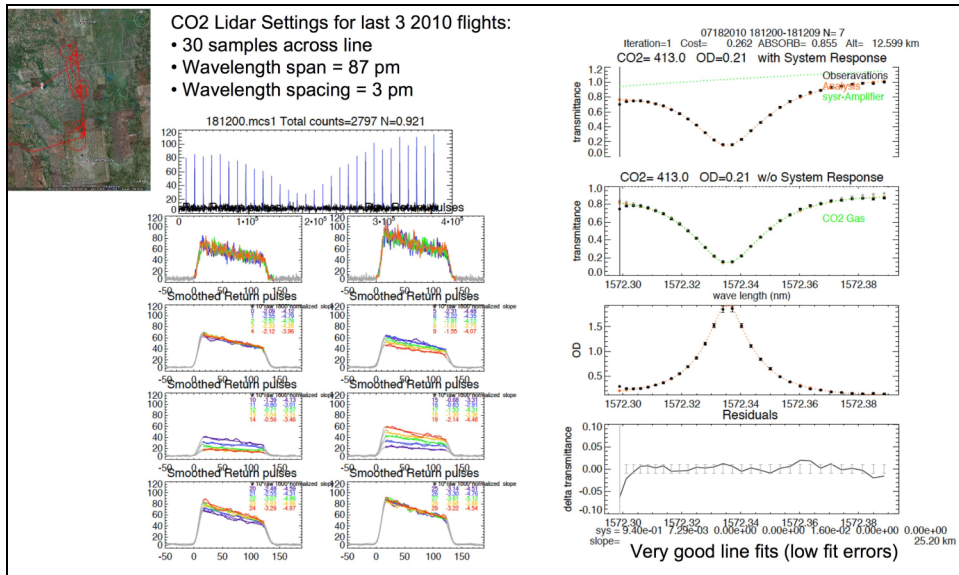


Figure 5 – (Left) A sample of a 1 second lidar backscatter record and some of the recorded pulse shapes from 12.5 km altitude from the flight over the DOE ARM site on July 18, 2010. (Right) Example fits of the computed CO2 line to the measurements in both transmission and optical depth units, and the errors in the fit vs wavelength.

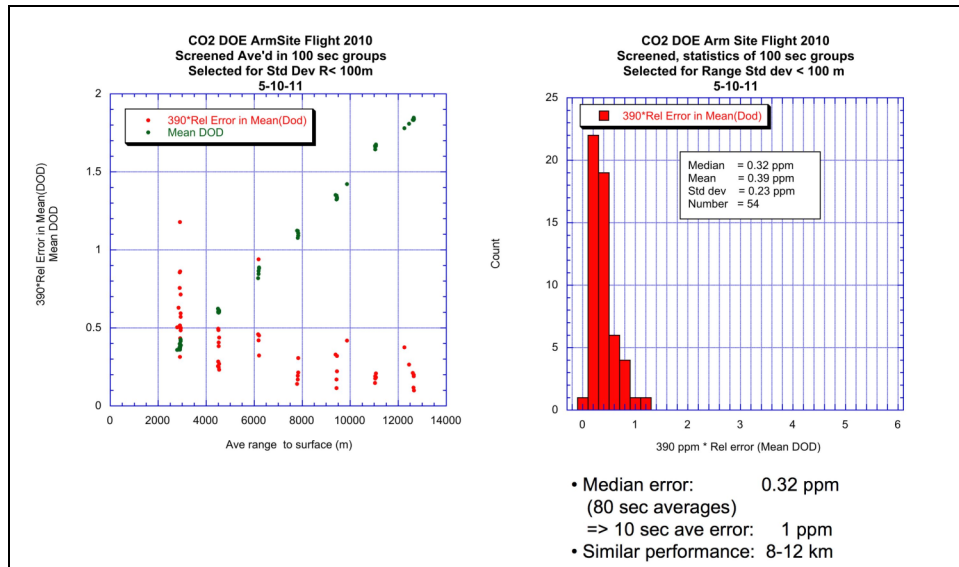


Figure 6 – Summary of measurements from the 2010 ARM site flight for 100 second segments where the range standard deviation was < 100m. (Left) Plots of DOD (green) and scatter (rms error) in the relative DOD, scaled to 390 ppm in red, vs range to the surface. The largest errors are at the lowest altitudes and most errors were < 0.5 ppm. (Right) Histogram of scatter in the relative error. The ave # of measurements was ~80 sec and median error was 0.32 ppm. For a shorter averaging time of 10 second the average error will scale to 1 ppm.

8. REFERENCES

- [1] United States National Research Council, "Earth Science and Applications from Space: National Imperatives for the Next Decade and Beyond," Available from <http://www.nap.edu/>. (2007).
- [2] NASA ASCENDS Mission Science Definition and Planning Workshop Report, Available from: http://cce.nasa.gov/ascends/12-30-08%20ASCENDS_Workshop_Report%20clean.pdf (2008).
- [3] Abshire, J. B., Riris, H., Allan, G. R., Weaver, C. J., Mao, J., Sun, X., Hasselbrack, W. E., Kawa, S. R. and Biraud, S., "Pulsed airborne lidar measurements of atmospheric CO₂ column absorption," *Tellus B*, no. doi: 10.1111/j.1600-0889.2010.00502.x (2010).
- [4] Krainak, M.A., et al., "Measurements of atmospheric CO₂ over a horizontal path using a tunable-diode-laser and erbium-fiber-amplifier at 1572 nm," in *Conference on Lasers and Electro-Optics, Technical Digest*, OSA, paper CTuX4, pages 878-881. ISBN: 1-55752-748-2 (2003).
- [5] J. B. Abshire, H. Riris, G. R. Allan, C. J. Weaver, J. Mao, X. Sun, W. E. Hasselbrack, A. Yu, A. Amediek, Y. Choi, and E. V. Browell, "A lidar approach to measure CO₂ concentrations from space for the ASCENDS Mission," *Proc. SPIE 7832*, 78320D (2010), DOI:10.1117/12.868567.
- [6] Stephen, M., Krainak, M., Riris H., and Allan, G. R., "Narrowband, tunable, frequency-doubled, erbium-doped fiber-amplified transmitter," *Optics Letters*, Vol. 32, No. 15 pages 2073-6 (2007).
- [7] Measures, R., *Laser Remote Sensing: Fundamentals and Applications*, Krieger Publishing, New York (1992).
- [8] Mao, J., Kawa, S. R., Abshire, J. B. and Riris, H., "Sensitivity Studies for a Space-based CO₂ Laser Sounder," *Eos Trans. AGU*, 88(52), Fall Meet. Suppl. Abstract A13D-1500(2007).
- [9] Y. Choi, S. Vay, K. Vadevu, A. Soja, J. Woo, S. Nolf, G. Sachse, et. al., "Characteristics of the atmospheric CO₂ signal as observed over the conterminous United States during INTEx-NA", *Journal of Geophysical Research*, 113, D07301, (2008).
- [10] A. Amediek et al., "Backscatter and Column Height Estimates from a pulsed airborne CO₂ Lidar," *ILRC-25 Conference Proceedings*, St. Petersburg Russia (2010).